Journal of Circuits, Systems, and Computers
Vol. 18, No. 3 (2009) 433–442

World Scientific
www.worldscientific.com

BODE-TYPE EQUALIZERS USING CURRENT CONVEYORS

AHMED M. SOLIMAN
Electronics and Communication Engineering Department,
Faculty of Engineering, Cairo University,
Giza 12613, Egypt
asoliman@ieee.org

Revised 30 October 2008

New voltage mode and current mode active RC Bode-type variable equalizers using current conveyors are introduced. The proposed equalizers can operate at much higher frequencies than the classical operational amplifier-based variable equalizers. Spice simulation results are included to confirm the practicality of the proposed circuits.

Keywords: Equalizers; current conveyors.

1. Introduction

Amplitude variable equalizers are used in many communication systems to compensate for deviations produced in the gain frequency characteristics of that system. Bode[1,2] introduced the basic design theory of variable magnitude equalizers and proposed passive RLC circuits, which were very useful in the past.

In the area of microelectronic circuits, the interest is in inductorless variable magnitude equalizers. Several variable active RC amplitude equalizers using the Operational Amplifier (op amp) as the active element have been introduced in the literature.[3–8] Due to the finite gain bandwidth product of the op amp, the amplitude equalizers realized using the op amp have limited frequency range of operation.

The objective of this paper is to generate new active RC variable amplitude equalizers to operate at higher frequency range. The active elements used are the Current Conveyor (CCII)[9] and the Modified Differential Current Conveyor (MDCCII).[10]

Bode[1,2] has shown that an acceptable approximation to the variable equalizer equation can be obtained by a transfer function of the form

$$T(s) = \frac{1 + xH(s)}{x + H(s)}\,. \tag{1}$$

The parameter x is usually chosen equal to R_v/R_o, where R_o is a suitable reference resistance and R_v is a variable resistance. Ideally x varies from 0 to infinity. This range $[0, \infty]$ is called the whole range of variation. $H(s)$ is a normalized driving point impedance function.

For $x = 0$, $T(s) = 1/H(s)$ and for $x = \infty$, $T(s) = H(s)$ and a flat response is obtained for $x = 1$.

Breglez[4] next showed that by mapping the range of the variable element in the classical Bode variable equalizer from $[0, \infty]$ to $[-1, +1]$ using the bilinear transformation given by

$$x = \frac{1+y}{1-y}\,. \tag{2}$$

The equalizer transfer function obtained is given by

$$T(s) = \frac{1 - yF(s)}{1 + yF(s)}\,, \tag{3}$$

where

$$F(s) = \frac{1 - H(s)}{1 + H(s)}\,. \tag{4}$$

For $y = -1$, $T(s) = 1/H(s)$ and for $y = +1$, $T(s) = H(s)$ and a flat response is obtained for $y = 0$.

The parameter y itself is now identified as the variable element. Equation (3) is realizable by the unsymmetrical passive lattice circuit shown in Fig. 1 which contains only a single shaping impedance. This lattice structure halves the range of variation of the variable element to $[0, +1]$ and does not permit simultaneous grounding of the input and the output.

Active circuits using one or two op amps were introduced in Refs. 4 and 5 to realize the half range and the full range variable amplitude equalizers.

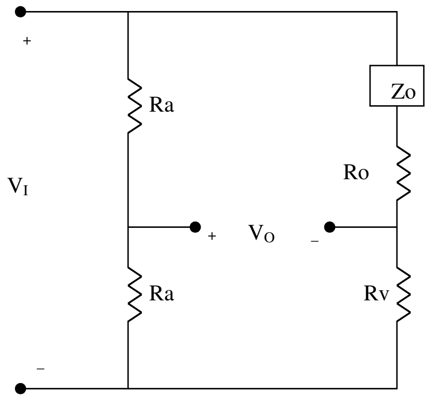

Fig. 1. The unsymmetrical passive lattice half range variable equalizer circuit.[4]

2. Half Range Equalizers Using CCII

Two new half range voltage mode variable equalizer circuits using CCII+ are introduced in Fig. 2. They are based on the op amp circuits in Ref. 4 using the transformation theorems given in Ref. 11. The circuit of Fig. 2(a) realizes an inverting transfer function given by

$$T(s) = -\frac{Z_o + R_o - R_v}{Z_o + R_o + R_v}\,. \tag{5}$$

This is in the form of Eq. (3) with $y = R_v/R_o$, $F(s) = R_o/(R_o + Z_o)$, which was realized in Ref. 4 using an op amp.

The circuit in Fig. 2(b) operates in open loop and replaces the floating resistor $2Ra$ connected between ports X and $Z+$ of the CCII in Fig. 2(a) by two grounded resistors connected to ports X and Z.

A noninverting transfer function can be achieved from the circuit of Fig. 2(b) using a CCII– instead of the CCII+. It should be noted that magnitude of the gain factor can be controlled by varying the grounded resistor connected to port Z.

Two new half range current mode variable equalizer circuits using CCII+ are introduced in Figs. 3(a) and 3(b). They are based on the CCII structures used in Refs. 12 and 13. Both circuits have current transfer functions of the form of Eq. (5). With CCII+ the circuit of Fig. 3(a) is noninverting and that of Fig. 3(b) is inverting. Of course CCII– can be used instead of the CCII+ and in this case the polarities will be reversed.

Two additional current mode circuits based on using the CCII+ as a Negative Impedance Converter (NIC) are given in Fig. 4.

Figure 5(a) introduces a new current mode variable equalizer based on using the MDCC introduced in Ref. 10 as the active element. An equivalent circuit using two opposite polarity CCs is given in Fig. 5(b). It is worth noting that similar structures to the basic structure of Fig. 5(b) were given in Refs. 14–16.

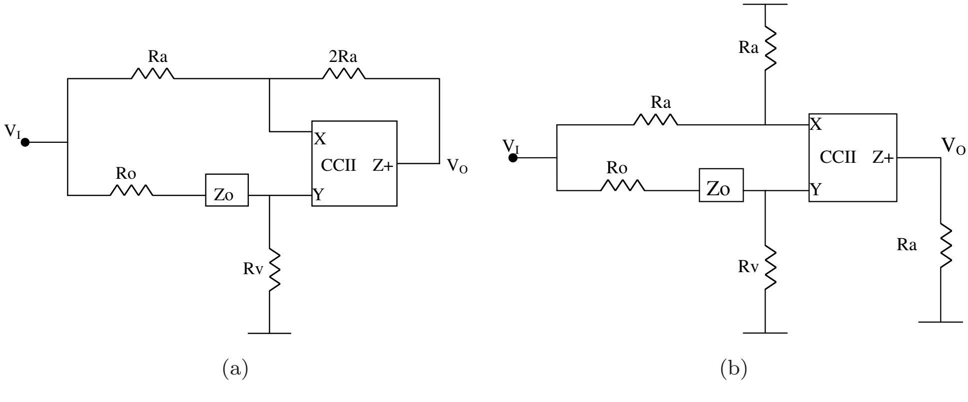

Fig. 2. (a) Half range variable equalizer voltage mode circuit using CCII+ and (b) variable equalizer voltage mode circuit using CCII.

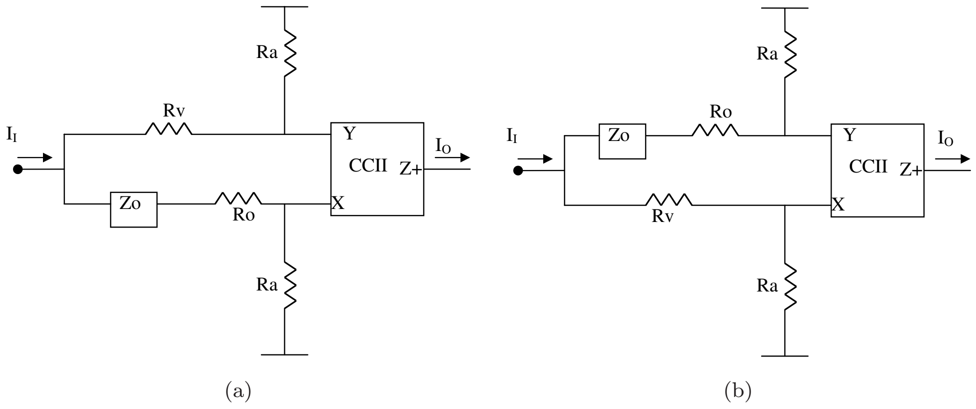

Fig. 3. (a) Noninverting current mode half range variable equalizer circuit using CCII and (b) inverting current mode half range variable equalizer circuit using CCII.

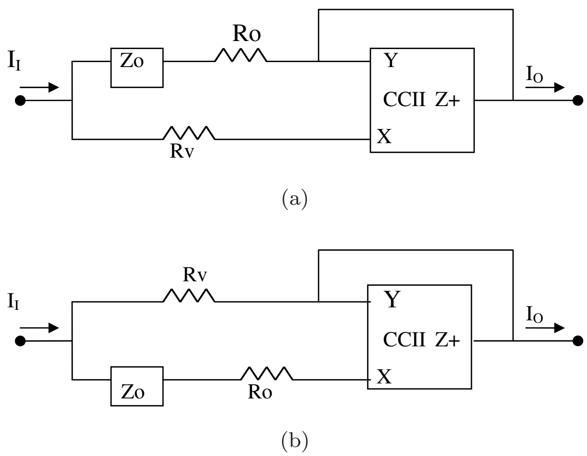

Fig. 4. (a) Current mode half range variable equalizer using CCII+ acting as NIC and (b) current mode half range variable equalizer using CCII+ acting as NIC.

3. Full Range Equalizers Using CCII

The circuit shown in Fig. 6(a) represents a voltage mode full range variable equalizer using a CCII+ which is generated from the op amp circuit given in Ref. 7 using the transformation theorem introduced in Ref. 11. The transfer function is given by

$$T(s) = \frac{Z_o(R_o + R_v) + 2R_o^2}{Z_o(R_o + R_v) + 2R_o R_v}\,. \tag{6}$$

This realizes the Bode type variable equalizer represented by Eq. (1), where $x = R_v/R_o$, $H(s) = Z_o/(Z_o + 2R_o)$.

For $R_v = 0$, $T(s) = 1 + [2R_o/Z_o]$ and for $R_v =$ Infinity, $T(s) = 1/[1 + (2R_o/Z_o)]$ and a flat response is obtained for $R_v = R_o$.

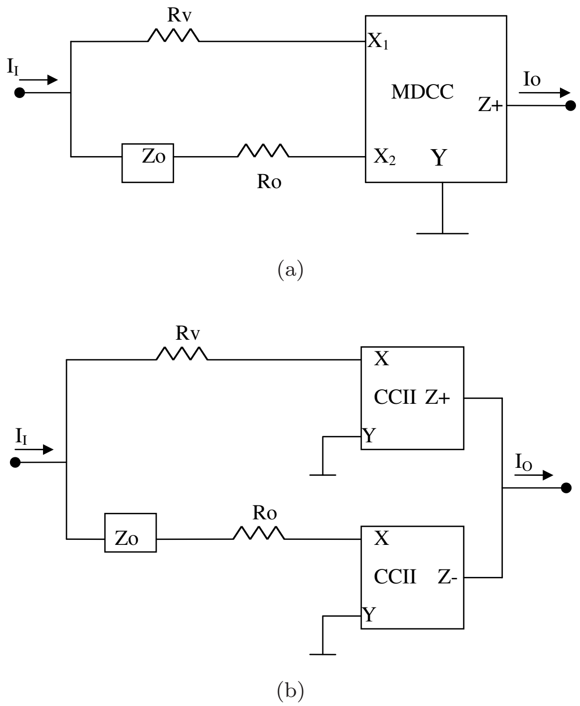

Fig. 5. (a) Current mode half range variable equalizer using MDCC and (b) current mode half range variable equalizer using CCII+ and CCII–.

The family of variable equalizers introduced in Ref. 8 is based on the transformation given by

$$x = \frac{Kb}{1-b}. \tag{7}$$

K is a real number greater than 1. From Eqs. (7) and (1) the following transfer function is obtained

$$T(s) = \frac{(1-b) + KbH(s)}{Kb + (1-b)H(s)}. \tag{8}$$

The full range of variation of this variable equalizer is when the control parameter b varies from zero to 1. For $b = 0$, $T(s) = 1/H(s)$ and for $b = 1$, $T(s) = H(s)$ and a flat response $T(s) = 1$ is obtained when $b = 1/[K+1]$.

Figure 6(b) represents an equivalent equalizer circuit which uses the CCII without feedback.

Figure 7(a) represents a new CCII+ realization of this variable equalizer with $K = 2$ and in this case the transfer function $T(s)$ is given by

$$T(s) = \frac{Z_o(R_o + R_v) + R_o(R_o - R_v)}{Z_o(R_o + R_v) + 2R_oR_v}. \tag{9}$$

A flat response is obtained when $R_v = R_o/3$ and $H(s) = Z_o/[Z_o + R_o]$.

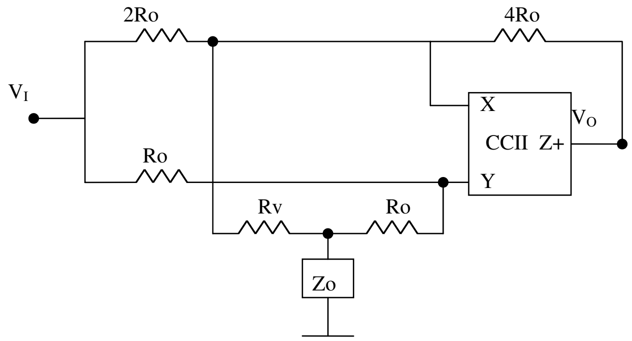

(a)

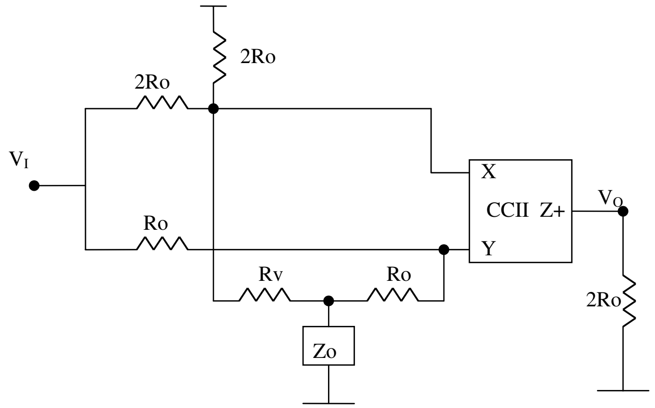

(b)

Fig. 6. (a) Full range variable equalizer circuit using single CCII+ and (b) full range variable equalizer circuit using single CCII+.

This circuit is related to the op amp circuit given in Ref. 8 by the transformation method reported in Ref. 11.

Figure 7(b) represents an equivalent equalizer circuit which uses the CCII without feedback. It can employ a CCII– and can provide magnitude gain by adjusting the grounded resistor connected to port Z.

4. Simulation Results

There are several types of variable amplitude equalizers based on the shaping impedance *Zo*. The bump equalizer uses a parallel RLC circuit[5] as the shaping impedance, or a series RLC circuit as the shaping impedance.[6,7] On the other hand, the fan equalizer uses a simple capacitor as the shaping impedance.

For simplicity only the fan equalizers will be simulated in this paper.

The AD844 with supply voltages of ± 5 V is used in the top Spice voltage mode simulations to follow.

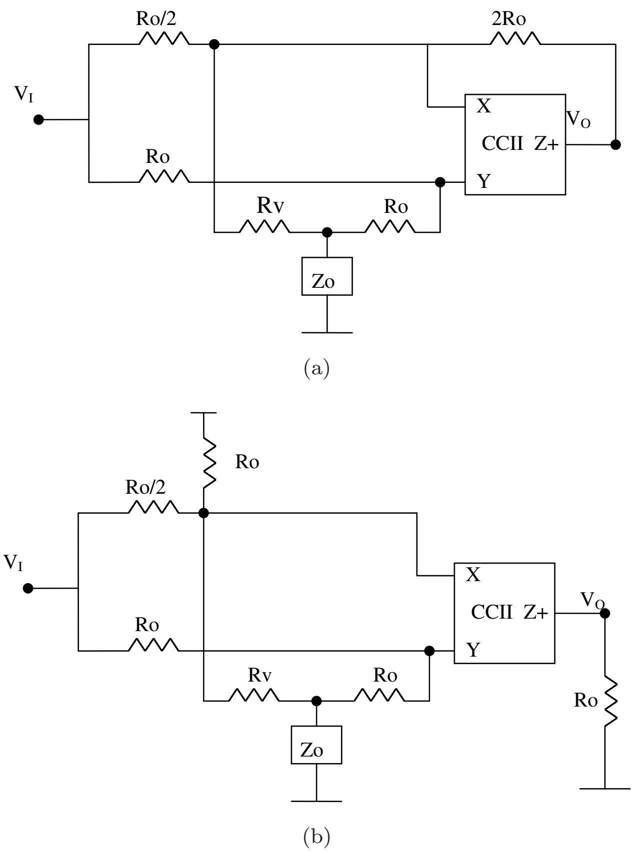

Fig. 7. (a) Full range variable equalizer circuit using single CCII+ and (b) full range variable equalizer circuit using single CCII+.

First the circuit of Fig. 2(b) is simulated with $R_o = 6\,\text{k}\Omega$, $R_a = 12\,\text{k}\Omega$, $C = 0.8\,\text{nF}$, and a 1 V sinusoidal input voltage source.

Figure 8(a) represents the simulated magnitude response for the half range with $R_v = 0$ and $R_v = R_o = 6\,\text{k}\Omega$.

The total power dissipation = 7.43 mW and THD = 2.232%.

The circuit of Fig. 6(b) is simulated with $R_o = 6\,\text{k}\Omega$, $C = 0.8\,\text{nF}$, and a 1 V sinusoidal input voltage source.

Figure 8(b) represents the simulated magnitude response for the full range with $R_v = 0$ and $R_v =$ Infinity, with a flat response for $R_v = R_o = 6\,\text{k}\Omega$.

The total power dissipation = 7.43 mW and THD = 2.1414%.

The circuit of Fig. 7(b) is simulated with $R_o = 12\,\text{k}\Omega$, $C = 0.8\,\text{nF}$, and a 1 V sinusoidal input voltage source.

Figure 8(c) represents the simulated magnitude response for the full range with $R_v = 0$ and $R_v = R_o = 12\,\text{k}\Omega$, with a flat response for $R_v = R_o/3 = 4\,\text{k}\Omega$.

The total power dissipation = 7.43 mW and THD = 2.077%.

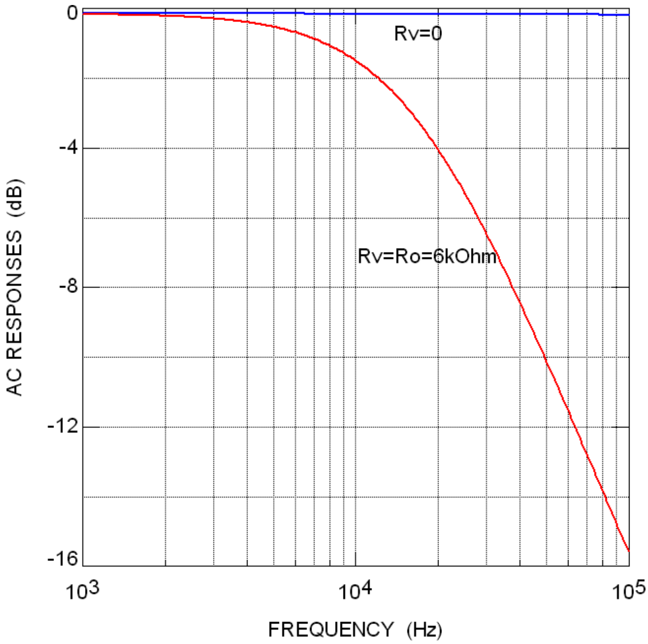

(a)

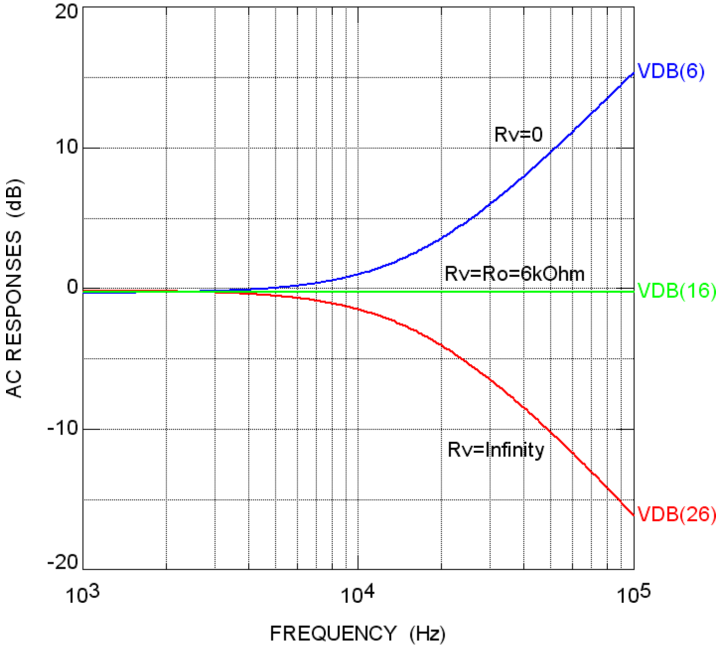

(b)

Fig. 8. (a) Simulated frequency response of the fan equalizer of Fig. 2(b), (b) simulated frequency response of the fan equalizer of Fig. 6(b) and (c) simulated frequency response of the fan equalizer of Fig. 7(b).

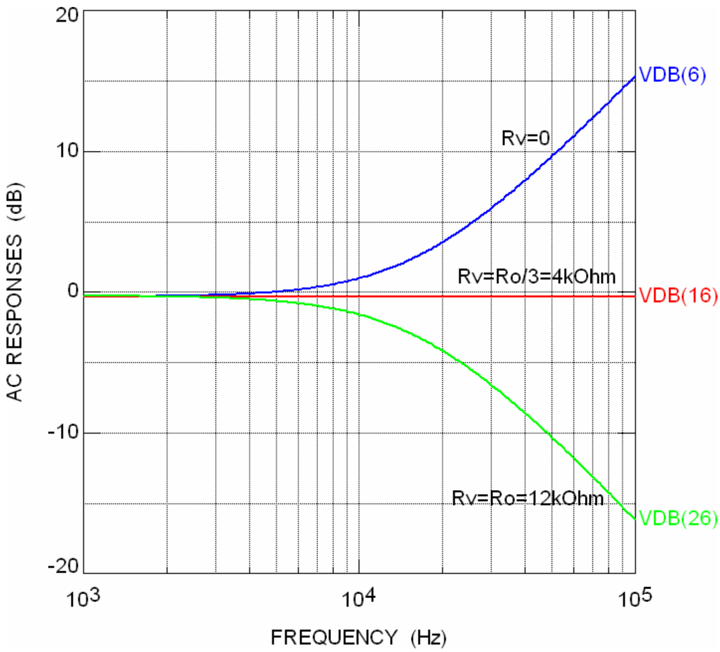

(c)

Fig. 8. (*Continued*)

5. Conclusions

New CCII and MDCC circuits for realizing variable amplitude equalizers are proposed. Current mode and voltage mode equalizers are proposed. Full range variable amplitude fan equalizers of the Bode type as used in Ref. 7 and of the transformed type as introduced in Ref. 8, are simulated using the commercially available AD844. Simulation results agree well with the theory.

References

1. H. W. Bode, Attenuation equalizer, *U.S. Patent 2 096 027* (1937).
2. H. W. Bode, Variable equalizers, *Bell Syst. Tech. J.* **17** (1938) 229–244.
3. P. E. Fleischer, Active adjustable loss and delay equalizers, *IEEE Trans. Circuits Syst.* **21** (1974) 527–531.
4. F. Breglez, Inductorless variable equalizers, *IEEE Trans. Circuits Syst.* **22** (1975) 415–419.
5. F. Breglez, Minimally active RC variable equalizers, *IEEE Trans. Circuits Syst.* **22** (1975) 688–691.
6. W. Saraga and M. Zyoute, A new active RC Bode-type variable equalizer circuit for microelectronic realization, *Proc. ISCAS, Houston* **2** (1980) 566–571.
7. M. Zyoute, New active RC Bode-type variable equalizer, *IEE Proc. G Electron. Circuits Syst.* **128** (1981) 134–137.
8. E. A. Talkhan, A. M. Soliman and T. H. El-Fayoumi, New family of active RC variable equalizers, *Electron. Lett.* **20** (1984) 497–498.

9. A. S. Sedra and K. C. Smith, A second generation current conveyor and its applications, *IEEE Trans. Circuits Theory* **17** (1970) 132–134.
10. H. O. Elwan and A. M. Soliman, CMOS differential current conveyors and applications for analog VLSI, *Analog Integr. Circuits Signal Process.* **11** (1996) 35–45.
11. A. M. Soliman, Theorem relating a class of op-amp and current conveyor circuits, *Int. J. Electron.* **79** (1995) 53–61.
12. A. M. Soliman, Theorem relating to port interchange in current mode CCII circuits, *Int. J. Electron.* **82** (1997) 585–604.
13. A. M. Soliman, Generation of current conveyor based all-pass filters from op-amp based circuits, *IEEE Trans. Circuits Syst. II* **44** (1997) 324–330.
14. S. I. Liu, D. S. Wu, H. W. Tsao, J. Wu and J. H. Tsay, Nonlinear circuit applications with current conveyors, *IEE Proc. G Electron. Circuits Syst.* **140** (1993) 1–6.
15. S. J. Azhari and H. Kaabi, AZKA cell, the current mode alternative of Wheatstone bridge, *IEEE Trans. Circuits Syst. I* **47** (2000) 1277–1284.
16. Y. H. Gallab and W. Badawy, A new topology for a current mode Wheatstone bridge, *IEEE Trans. Circuits Syst. II* **53** (2006) 18–22.